Kinetics of the RNA−DNA Helicase Activity of *Escherichia coli* Transcription Termination Factor Rho. 1. Characterization and Analysis of the Reaction†

Katherine M. Walstrom, Jody M. Dozono, Srebrenka Robic,‡ and Peter H. von Hippel*

Institute of Molecular Biology and Department of Chemistry, University of Oregon, Eugene, Oregon 97403

Received December 27, 1996; Revised Manuscript Received April 24, 1997⊗

ABSTRACT: The kinetics of the ATP-dependent RNA−DNA helicase activity of *Escherichia coli* transcription termination factor rho have been analyzed. Helicase substrates were assembled using 255 nt and 391 nt RNA sequences from the *trp t′* RNA transcript of *E. coli*. These RNA sequences each carry a rho "loading site" at a position near the 5′-end, and a rho-dependent terminator sequence at the 3′-end to which complementary ∼20 nt DNA oligonucleotides have been annealed. A rapid (∼ 30 s) pre-steady-state burst of helicase activity (DNA oligomer release), followed by a slow linear phase, is observed in reactions carried out at low salt concentrations (50 mM KCl). Using poly(rC) or poly(dC) as traps for the rho that is released after one round of activity, we have shown that the first (burst) phase of the reaction represents the processive translocation of prebound rho hexamers from the rho loading site to the 3′-end of the RNA molecule. The slow phase of the reaction is complex and represents a combination of many different processes, including the slow release of RNA from rho, the reannealing of complementary DNA oligonucleotides to the RNA substrate, and the recycling of rho hexamers onto additional RNA molecules. Reactions carried out at higher salt concentrations (150 mM KCl) consist of only one phase, since under these conditions rho dissociates more rapidly from the RNA, with an amplitude corresponding to several DNA oligomers removed per rho hexamer. Thus, rho can recycle and function as a catalytic helicase under reaction conditions resembling those found in the cell.

Transcription termination factor rho of *Escherichia coli* is required to release nascent RNA[1] transcripts at rho-dependent termination sites on the DNA template (for reviews, see ref *1*−*5*). The mechanism of this rho- and ATP-dependent RNA-release process is not understood, but it has been shown that rho can function as a specific (5′ → 3′) RNA−DNA helicase *in vitro* (*6*). On this basis, it has been widely assumed that one of the major roles of rho in rho-dependent transcription termination is to separate the RNA−DNA hybrid involved in the interaction of the 3′-end of the nascent RNA with the DNA template within the transcription complex. Recent evidence for the presence of an RNA−DNA hybrid in elongation complexes that is ≥9 bp in length is presented in Nudler et al. (*7*).

Rho functions as a hexamer of genetically identical 47 kDa subunits (*8*, *9*), which are arranged in the functional rho complex as a hexagonal trimer of asymmetric dimers (*9*−*12*). In this form, rho binds single-stranded RNA, which activates the ATP hydrolase activity of the protein (*8*, *13*). Rho-dependent terminators are characterized by an upstream region on the template that encodes an RNA sequence that is 60−100 nt in length, is largely devoid of secondary structure, and is relatively rich in cytosine residues (*14*−*16*). This region is called the rho-loading site and binds rho preferentially in competition with other sequences along the nascent transcript (*17*).

Most current models of rho-dependent termination argue that rho, due to its single-stranded RNA binding character, binds effectively to the transcript at this loading site. This binding then activates the RNA-dependent ATPase activity of the protein (*18*), which in turn fuels the movement of the rho hexamer along the RNA in a 5′ → 3′ direction (for recent structure-based models of this process, see ref *5*, *19*). Rho-dependent transcript termination seems to occur at sites at which the elongating transcription complex pauses on the template (*20*−*23*). This pausing does not depend on the presence or action of rho, but is an intrinsic property of the polymerase, reflecting its interaction (either direct or via the nascent RNA) with pause-inducing sequences along the template. Pausing of the transcription complex is thought to favor rho-dependent termination primarily because the probability of rho completing its 5′ → 3′ translocation along the nascent RNA from the loading site, and thus "catching-up" with the transcription complex (*23*, *24*), is highest at these pausing positions.

One model for rho-dependent termination, sometimes called kinetic coupling, suggests that the efficiency of rho-dependent termination is partially determined by the relative rates at which rho translocates (5′ → 3′) along RNA and RNA polymerase translocates (3′ → 5′) along the template

† This research was supported in part by U.S. Public Health Service Research Grants GM-15792 and GM-29158 (to P.H.v.H.), by NIH Individual National Research Service Award GM-16069 (to K.M.W.), and by a grant to the Institute of Molecular Biology at the University of Oregon from the Lucille P. Markey Charitable Trust. P.H.v.H. is an American Cancer Society Research Professor of Chemistry.

* To whom correspondence should be addressed. Telephone: 541-346-5151. FAX: 541-346-5891. E-mail: petevh@molbio.uoregon.edu.

‡ Present address: Department of Biology, Beloit College, Beloit, WI 53511.

⊗ Abstract published in *Advance ACS Abstracts,* June 15, 1997.

[1] Abbreviations: ATP, adenosine 5′-triphosphate; ATPase, adenosine-5′-triphosphate hydrolase; bp, base pair(s); CTP, cytidine 5′-triphosphate; DEAE, diethylaminoethyl; DNA, deoxyribonucleic acid; DTT, dithiothreitol; EDTA, ethylenediaminetetraacetic acid; Glu, glutamate; GTP, guanosine 5′-triphosphate; HEPES, *N*-(2-hydroxyethyl)piperazine-*N*′-2-ethanesulfonic acid; nt, nucleotide(s); NT, nitrocellulose; OAc, acetate; poly(dC), poly(deoxycytidylic acid); poly(rC), poly(cytidylic acid); rC, ribocytidine; RNA, ribonucleic acid; SDS, sodium dodecyl sulfate; Tris, tris(hydroxymethyl)aminomethane; UTP, uridine 5′-triphosphate.

S0006-2960(96)03179-0 CCC: $14.00 © 1997 American Chemical Society

strand of the DNA genome. Early experiments showed that changing the rate of elongation of the RNA polymerase (either by adding λ Q antitermination protein or by using a mutant RNA polymerase) changed the efficiency of rho-dependent termination (*25*, *26*). This model gained further support because partially defective rho proteins could regain function in combination with slow RNA polymerase mutants (*24*). These results, in addition to the importance of elongation complex pause sites described above, support the idea that the rate of translocation of rho is important for its function.

Using appropriate model substrates, Platt and co-workers showed that rho can operate as an ATP-dependent (5′ → 3′) RNA−DNA helicase to separate RNA−DNA duplexes if the hybrid duplex is formed at the 3′-end of a single-stranded RNA transcript that carries a rho loading site (*6*, *27*). However, these early measurements revealed a helicase reaction that seemed very slow, consumed a large amount of ATP, and was stoichiometric (rather than catalytic) in rho concentration, since the number of duplexes separated was always equal to or less than the number of rho hexamers present (*27*−*29*). Assuming that some of these properties might be "improved" by operating under other reaction conditions, we set out to further characterize the properties of rho as a helicase, based on the premise that understanding this activity should yield significant information on how rho translocates directionally along RNA, how it unwinds double-stranded nucleic acid sequences, and thus how it might function in transcript termination. Some of our results are described here and in the companion paper (*30*).

In this paper, we show that the rho helicase reaction is characterized by a rapid, pre-steady-state burst of helicase activity under low salt concentration conditions (50 mM KCl), and that this phase corresponds to the first round of 5′ → 3′ translocation of the rho hexamer along the RNA transcript from the rho loading site to the 3′-terminus. This rapid phase is followed by a slower phase that reflects a mixture of secondary reactions, including the slow release of RNA from rho, the reannealing of DNA oligomers to the RNA substrate, and the recycling of rho onto other RNA substrates. Under these conditions, the helicase reaction indeed appears to be stoichiometric, since rho is released from the RNA transcript only very slowly (compared to the rate of translocation of rho along RNA) following completion of the RNA−DNA hybrid separation process. We also show here that rho can act as a catalytic helicase if the reaction is carried out at higher salt concentrations (∼150 mM KCl). Under these conditions, rho releases RNA rapidly and, as a consequence, can recycle to other RNA substrates. In the companion paper (*30*), we then use the helicase assay, in combination with ATPase assays and rho−RNA binding measurements performed under the same conditions, to analyze the rate and processivity of the ATP-dependent translocation of rho along the RNA transcript. Finally we present a mechanistic model for rho helicase activity and consider how these functional properties might be manifested in rho-dependent transcription termination.

MATERIALS AND METHODS

Preparation of Rho Protein. Wild-type rho protein was obtained from *E. coli* strain AR120/A6, which carries the rho overexpression plasmid p39ASE (*31*). The overexpression vector that was used in many earlier studies of rho is now known to contain a point mutation, although the properties of this mutant rho are very similar to those of the wild-type protein (*31*; K.M.W., unpublished results). The corrected plasmid (p39ASE), which was a generous gift from Professor Terry Platt at the University of Rochester, was used to overexpress the rho protein used in these experiments.

Rho protein was purified as described previously (*9*), except that the purification was stopped after the heparin−agarose column. Thus, the agarose−5-[(4-aminophenyl)-phosphoryl]uridine 2′(3′)-phosphate column and the Bio-Gel A5M columns used in the earlier preparation were omitted, since we found that after the heparin−agarose column the protein was already >99% pure as defined by silver staining of SDS−polyacrylamide gels. Stock solutions containing rho protein at hexamer concentrations in excess of 2 μM were stored at −20 °C in rho storage buffer, containing 50% glycerol, 20 mM Tris-HCl (pH 7.9), 100 mM KCl, 0.1 mM EDTA, and 0.1 mM dithiothreitol (DTT). Rho concentrations were determined by the UV absorption at 280 nm, using a molar extinction coefficient of 1.5×10^4 M^{-1} cm^{-1} per monomer (*9*). Unless otherwise indicated, rho protein concentrations are expressed in units of hexamers throughout this and the companion paper (*30*).

Rho stock solutions were diluted into reaction buffer less than 5 min before the start of each experiment. This timing was important because rho hexamers can dissociate slowly to monomers at low protein concentrations (*9*) and thus lose ATPase (and presumably helicase) activity (data not shown). Rho preparations were tested for activity by titrating the protein with RNA_{255} (see Figure 1A for helicase substrate nomenclature), which contains the *trp t′* rho loading site. Rho protein binds to this RNA with a 1 (±0.2) RNA molecule per rho hexamer stoichiometry at rho hexamer concentrations less than 1 nM (data not shown; our binding assay procedures are described below). Results in Walstrom et al. (*30*) also show that all the bound rho is fully active as a helicase and in hydrolyzing ATP. Thus, by these criteria, our rho protein preparations are 100% active.

Templates for RNA Production. The *trp t′* rho-dependent terminator, positioned on plasmid pWU5 (*32*), was also a generous gift from Professor Terry Platt. The pWU5 plasmid was cut with *Hinc*II, yielding a 212 bp fragment containing the rho loading site and the termination region. The fragment was ligated into *Hinc*II-cut pGEM3Zf(+) (Promega), yielding pGEMtrpt1′. This plasmid carries the coding sequence for the *trp t′* terminator positioned downstream of an SP6 promoter. One transcription template was prepared by cutting this plasmid with *Pvu*II and *Bam*HI, yielding a 443 bp fragment that encodes a 255 nt RNA sequence containing the entire *trp t′* termination region (RNA_{255}, see Figure 1A). A second template was prepared by cutting the plasmid with *Pvu*II, yielding a 588 bp fragment that encodes a 391 nt RNA sequence containing the *trp t′* region and downstream plasmid sequences containing part of the *lacZ* coding sequence (RNA_{391}, Figure 1A). The transcription templates were purified in NuSieve GTG low-melt agarose (FMC) and isolated using β-agarase (NEB).

RNA Synthesis. In vitro transcription of RNA was carried out in 25 μL volumes containing 40−50 nM concentrations of transcription template, 100 μg/mL acetylated bovine serum albumin (USB), 10 mM DTT, 1 mM ATP, 1 mM UTP, 1 mM GTP, 100−500 μM CTP, 20 mM HEPES (pH 7.9), 6

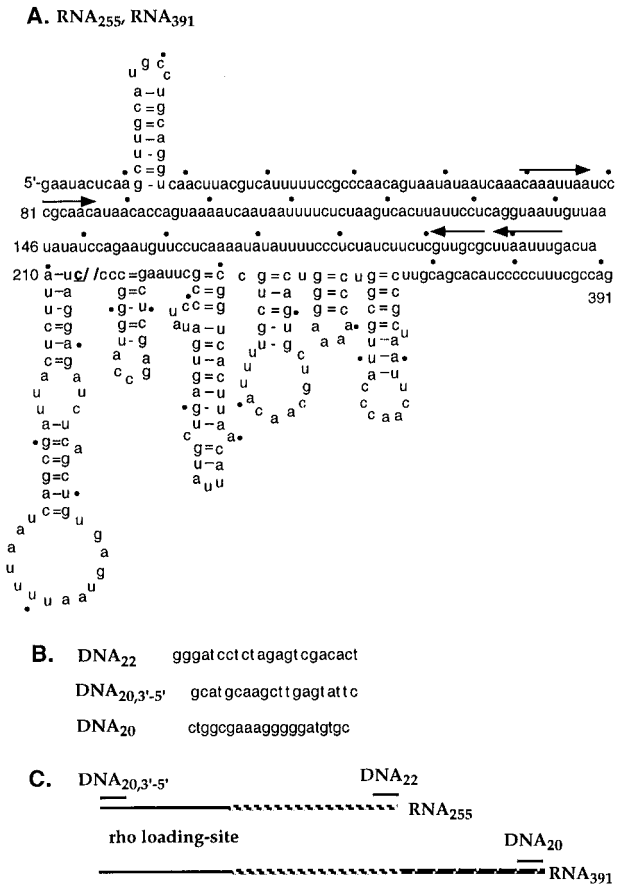

FIGURE 1: RNA and DNA substrates. The name of each molecule (in boldface type) indicates its length and composition. For example, RNA_{255} is 255 nt in length. (A) Sequences of RNA_{255} and RNA_{391}. Included are the predicted secondary structures of RNA hairpins with free energies less than −1.0 kcal/mol at 37 °C, as determined by the MFOLD program of the GCG, Wisconsin Package (version 8.0, Genetics Computer Group). The arrows indicate a possible hairpin with a very large loop that has a free energy of −6.9 kcal/mol, if formed. The solid circles mark 10 nt spacings along the sequence. The end of the RNA_{255} molecule is indicated by the boldface double slashes. Residue 255 is indicated by the boldface underlined c. (B) Sequences (5′ → 3′) of the DNA oligomers used in these experiments. The 3′−5′ subscript on the second oligomer denotes the direction (relative to the RNA) of the helicase reaction required to remove it. (C) Annealing positions of the DNA oligomers on the RNA component in forming the various helicase substrates. Long lines designate RNA, with the narrow section corresponding to the rho loading site. RNA segments with the same sequence are shown with the same shading pattern. Short lines designate DNA and are placed next to the RNA sequences to which they anneal. The lengths of the lines are proportional to the size of the actual oligomers. The RNA component of the helicase substrate is described in detail under Materials and Methods. The corresponding trapping DNA oligomers are all 20 nt in length and are complementary to 20 nt of each DNA oligomer that anneal to the RNA.

mM $MgCl_2$, 2 mM spermidine, 1.1 units/μL RNasin (Promega), 50 μCi of [α]-^{32}P]CTP (DuPont−NEN, 3000 Ci/mmol), and 2 units/μL SP6 RNA polymerase (NEB, Promega, or USB). Reactions were incubated at 40 °C for 1 h, and then 10 units of DNase I (USB) and 1.5 units/μL RNasin were added to the reaction, followed by incubation at 37 °C for an additional 15 min. The reaction was diluted to 200 μL with HE buffer (5 mM HEPES-Cl, pH 7.9, and 0.1 mM EDTA), phenol−chloroform-extracted twice, and then subjected to one or two cycles of chloroform extraction. The reaction was placed in the top reservoir of a Centricon 100 filtration device (Amicon), diluted to 0.5 mL, and filtered with air pressure until 100−200 μL remained. Then 1.5−2 mL of HE buffer was added, and the resulting solutions were filtered until 100−200 μL remained. These last dilution and filtration steps were repeated 2 more times. The solution was recovered from the Centricon device and stored at 4 °C. The concentrations of the various RNAs synthesized were calculated from the specific activity of CTP in the transcription reaction solution, the amount of radioactivity incorporated into each RNA in the purified solution, and the number of rC residues in the RNA; 85−90% of the radioactive molecules were within ±1 nt of full-length (from promoter to terminator) as defined in Figure 1A.

Phage polymerases can also initiate transcription at the ends of templates and thus can synthesize RNA transcripts that are the same length as the entire template. Less than 1% of the radioactivity in our RNA_{255} preparations was incorporated into long RNA molecules that could result from end-to-end transcription of the DNA template. Since such end-to-end transcripts would contain more rC residues per molecule than would the expected RNA_{255}, the number of end-to-end transcripts obtained was less than 1% of the RNA_{255} product. The purified RNA_{391} preparation contained ∼10% of the radioactivity in the form of a long end-to-end transcription product. These longer RNA molecules were well separated from the RNA_{391} bands on the helicase gels (see below), so they did not affect the data analysis. Both preparations were used without further purification. The final RNA preparations were end-labeled with polynucleotide kinase (New England Biochemicals) and run on a denaturing, polyacrylamide gel to show that the preparations contained no DNA template fragments.

Polynucleotides and DNA Oligomers. Poly(rC) and poly(dC) were purchased from Pharmacia. Concentrations of poly(rC) were measured using the UV absorbance at 268 nm with a (per residue) extinction coefficient of 6.2×10^3 M^{-1} cm^{-1} (*33*). Concentrations of poly(dC) were measured by the absorbance at 274 nm, using an extinction coefficient of 7.4×10^3 M^{-1} cm^{-1} (*34*). Poly(rC) samples were fractionated on Sepharose 4B (Sigma), end-labeled with polynucleotide kinase, and sized by denaturing polyacrylamide gel electrophoresis. All fractions used in our experiments exceeded 300 nt in length. Poly(dC) was stored at −20 °C as 0.1−1.0 mM stock solutions in 5 mM HEPES-Cl, pH 7.9, and 1 mM EDTA. Poly(dC) samples were not fractionated, since the average chain length of the preparations was 280 nt (determined by Pharmacia). Stock solutions of poly(dC) were checked for precipitation prior to use, since the solubility limit of this material in the buffer used was ∼0.2 mM (in nucleotide residues). If precipitation was observed, the solutions were heated to 70−90 °C, mixed well, and diluted to a final concentration of 0.1 mM.

The DNA oligonucleotides used in preparing helicase substrates (and complementary "trapping" DNA oligomers) were obtained from Genosys (The Woodlands, TX), Midland (Midland, TX), or Bio-Synthesis (Lewisville, TX). Some preparations of DNA oligonucleotides were purified using denaturing polyacrylamide gel electrophoresis. More than 95% of the DNA oligomers used in our studies were within 1 nt of the specified length, and no more than 10% of any sample was 1 nt longer or shorter than full-length. The sequences and designations of the DNA oligonucleotides used are shown in Figure 1B.

Assembly of Helicase Substrates. RNA chains at a final concentration of 50 nM were mixed in annealing buffer with 80 nM (100 nM for DNA_{20}) concentrations of DNA oligomers complementary to sequences at the 3′ (or 5′) ends of the RNA (see Figure 1C). The annealing buffer contained 20 mM HEPES-Cl (pH 7.9), 150 mM KCl, and 0.1 mM EDTA. Mg^{2+} was specifically excluded from the annealing mixture to prevent Mg^{2+}-dependent degradation of the RNA, which we have observed at high temperatures (K.M.W., unpublished results). Solutions were heated to 95−100 °C for 3−5 min and then slowly cooled (at ∼1 °C/min) to room temperature to promote proper hybridization. Annealing mixtures for the catalytic helicase experiments (Figure 6) contained 100 nM RNA_{255} and 160 nM DNA_{22}. After annealing, the solutions were stored at 4 °C. The excess DNA oligonucleotides present in these mixtures were not removed, because they were bound (trapped) by the complementary trapping DNA oligomers present in the helicase reactions (see below).

Helicase Assays. Most of our helicase assays were performed in helicase buffer containing 20 mM HEPES-Cl (pH 7.9), 50 mM KCl, 1 mM $Mg(OAc)_2$, 0.1 mM EDTA, and 0.1 mM DTT, in a total reaction volume of 35 μL. The annealed RNA−DNA helicase substrates were diluted to a final concentration of 10 nM (in molecules). The KCl concentration of the helicase buffer stock solution was adjusted so that the total KCl concentration after addition of the annealed RNA−DNA substrates was either 50 mM or 150 mM (see Results). The helicase reactions also contained 60 nM concentrations of DNA "trapping" oligomers. These trapping oligomers had sequences complementary to the DNA oligomers initially annealed to the RNA, and they served to trap these latter DNA oligomers as they were released by the helicase, thus preventing re-formation of the helicase substrate.

In most experiments, rho was added to the reaction and allowed to bind to the RNA for 1−5 min before initiating the reaction by adding 1 mM ATP. In reactions containing a poly(rC) or poly(dC) rho trap (see below), the poly(rC) or poly(dC) was added with the ATP at zero time. Aliquots (5 μL) of the reaction were removed after various times of incubation and added to 2−3 μL of gel loading buffer (20% Ficoll 400, 0.1 M EDTA, pH 8.0, 1% SDS, 0.25% bromphenol blue, and 0.25% xylene cyanol) to stop the reaction. Since the gel buffer contains SDS, rho is denatured when the helicase assay sample is mixed with loading buffer.

Gel Electrophoresis. Helicase reactions, run for various lengths of time and stopped as above, were separated on Laemmli-type discontinuous polyacrylamide gels. The running gel was 5 in. long and 0.75 mm thick and contained 5.5% acrylamide [19:1 acrylamide:bis(acrylamide) ratio], 0.375 M Tris-HCl (pH 8.8), 1% SDS, and 2 mM EDTA. The stacking gel was 1.5 in. long and 0.75 mm thick and contained 0.125 M Tris-HCl (pH 6.8), 4% acrylamide (19:1), 1% SDS, and 2 mM EDTA. Gels were run at 25 mA for 2 h, dried, and analyzed as described below. RNA_{391} helicase substrates were run under the same buffer and running conditions as the RNA_{255} substrate, except that the running gel contained 4% acrylamide and was 10 in. long.

This discontinuous gel system could separate the free RNA from the remaining annealed RNA−DNA duplexes without smearing the RNA bands (e.g., see Figure 2), because the SDS in the gel buffer prevents retention of RNA in the well and retardation on the gel. RNA smearing in the gel observed in the absence of SDS may have been caused by rho that bound to RNA after the samples had entered the gel. All RNA−DNA hybrids used in these studies were stable in the gel (see Results), and the presence of EDTA prevented nuclease degradation of the nucleic acid components.

The above procedures were required to permit the acquisition of consistent quantitative data in these helicase assays. We first attempted to monitor the release of radioactively-labeled DNA oligomers to follow the progress of the helicase reaction. Data obtained by this procedure were not consistent, since measuring the extent of the helicase reaction in this way depended on knowing the specific activity of each polynucleotide and the volume of sample loaded onto each lane. Errors in any of these measurements affected the results. In addition, end-labeled DNA oligomers were not used since they seemed to degrade within 1−2 weeks.

We therefore used only radioactively-labeled RNA in our experiments, because the incorporation of ^{32}P into the RNA during transcription provided the most sensitive measure of RNA concentration, and also because this procedure allowed us to assess the integrity of the RNA in each experiment. Results obtained with labeled RNA were reproducible over multiple RNA preparations. Another advantage of using labeled RNA is that the fraction of RNA annealed to DNA in each lane is independent of the specific activity of the RNA and of the volume of the sample loaded into each lane.

Quantitation of the Helicase Reactions. Gel electrophoresis of each helicase reaction sample resulted in clean separation into two radioactive bands, corresponding to free (released) RNA and to RNA still annealed to the complementary DNA oligomer (Figure 2). The fraction of radioactivity contained in each band was determined in one of three ways. In most experiments, the gels were scanned with an AMBIS 4000 Radioanalytic Imaging Detector (Scanalytics, Inc.). Some gels were scanned with a Molecular Dynamics Storm 860 Phosphorimager. In a few experiments, the bands were cut out of the gel and quantitated by liquid scintillation counting.

In the experiments with the RNA_{255} helicase substrate, the initial substrate seemed to consist entirely of RNA annealed to the appropriate complementary DNA oligomers (see Figure 2). Yet when the starting fraction was quantitated as above, it showed only 90−95% annealing, even after subtracting background radioactivity. (Background was measured in an area of the gel located directly below the position of the free RNA band.) This apparent limiting level of annealing was obtained even when no free RNA band could be detected on film. The background radioactivity remaining in the lanes in which all the RNA should have been annealed may have been caused by RNA products shorter than the major full-length product, which would have formed less stable complexes than the full-length material. This is consistent with the observation that ∼10% of the radioactivity in our RNA preparations was present as RNA molecules that were shorter than full-length (see above) and with the fact that a slight smear of radioactivity is evident at positions at which shorter RNA bands would be expected to run in the gel (see Figure 2). No background radioactivity was seen in the gel at positions above the free RNA band, meaning that no radioactive molecules longer than the full-length RNA were present. Since we are not entirely sure of

the origins of this small discrepancy, the helicase results were calculated on the basis of an initially annealed RNA fraction of 0.9−0.95. The RNA_{391}/DNA_{20} annealing mixtures contained 90% of the radioactivity in the annealed band. This fraction could not be increased, even by increasing the concentration of DNA_{20}, so these data were calculated on the basis of an initially annealed RNA fraction of 0.90.

The measured fraction of RNA annealed to DNA for each sample was plotted versus time, and all of the data points [for experiments performed in the absence of trapping poly(rC) or poly(dC)] were fit to the sum of one fast exponentially-decaying component and one slow linearly-decaying component, as follows:

$$F = A_1 \exp(-k_1 t) + (A_2 - k_2 t) \quad (1)$$

where F represents the fraction of RNA annealed to DNA at time t, A_1 and k_1 are the amplitude and rate constant, respectively, of the exponential (burst) phase of the helicase reaction, and A_2 and k_2 are the intercept and slope, respectively, of the slow linear phase. Data obtained in the presence of poly(rC) or poly(dC) rho traps, or in reactions with similar concentrations of RNA and rho hexamers in buffers containing 150 mM (rather than 50 mM) KCl, were fit to the sum of one exponentially-decaying component plus a constant term (i.e., $k_2 = 0$), because in these reactions the second phase was flat over the entire time course of the experiment.

Filter-Binding Assays To Measure Rho−RNA Binding. Filter-binding assays to measure RNA binding to rho were performed as described (*35*). Samples containing helicase buffer (see above), 0.2−20 nM RNA molecules, and 0.2−20 nM rho hexamers (added last) were prepared and then incubated at room temperature (22 °C) for 5−10 min before applying 5 μL samples to nitrocellulose (BA85, Schleicher & Schuell) and DEAE (NA45, Schleicher & Schuell) filters contained in a modified Minifold filtration apparatus (Schleicher & Schuell, modification instructions in ref *35*). Solutions were prepared in the absence of ATP, and ATP was added to some samples less than 1 min before filtering. The addition of ATP diluted the solutions by less than 7% of the total volume. The filters were dried and scanned on an AMBIS 4000 Radioanalytic Imaging Detector, or the spots were cut out and counted in a liquid scintillation counter. The fraction of radioactive RNA bound (F_{bound}) to nitrocellulose was calculated as

$$F_{bound} = \frac{cpm_{NT}}{cpm_{NT} + cpm_{DEAE}} \quad (2)$$

where cpm_{NT} are the counts per minute measured on the nitrocellulose (NT) filter and cpm_{DEAE} are the counts per minute measured on the DEAE filter for each sample, respectively. Control reactions containing no protein showed binding (to the NT filter) of less than 0.1% of the RNA (data not shown).

RNA Release Rate Determinations. Rho and RNA solutions (0.5 nM RNA and 2 nM rho, containing either 50 or 150 mM KCl) were diluted 10-fold into helicase buffer containing 50 or 150 mM KCl, respectively. The fraction of RNA bound to rho before dilution was determined using a 10 μL sample from the original binding mixture, and 100 μL aliquots were taken from the diluted reaction samples. The fraction of RNA bound in each sample was determined as described for the filter-binding assays (above) and plotted against reaction time. The data obtained at 150 mM KCl salt concentrations were fit to the sum of two exponentially-decaying functions. A single-exponential fit could not be used because the curve did not go through the 10 min data points for either curve (plots not shown, rates in Results), and the single-exponential fit showed a χ^2 value that was twice as large as that obtained by fitting the same data to two exponential components. The data measured in 50 mM KCl were very scattered because the fraction of RNA bound to the nitrocellulose filters did not change much with time, even after 20 min of reaction. The data were plotted semi-logarithmically against time, and initial slopes were used to determine dissociation rates.

RESULTS

The rho-catalyzed RNA−DNA helicase reactions described here were performed with essentially the same RNA component of the helicase substrate (the *trp t′* transcript) that was used by Platt and co-workers to initially characterize the rho helicase activity (*6*, *27*). However, in our studies, we hybridized short DNA oligomers to sequences at the 3′-end of the RNA to form the helicase substrates, rather than annealing the RNA to complementary sequences of entire large single-stranded plasmid DNA circles (see ref *6*). In the first stages of our study, we show that the helicase reaction in our hands displays the fundamental properties observed earlier (*6*, *27*). We then present a quantitative study of the kinetics of the reaction. To this end, we have developed the gel system described under Materials and Methods to allow us to determine, with a high degree of reproducibility, the amount of RNA that remains annealed to the hybridized DNA oligomers at different stages of the reaction.

Characterization of the RNA−DNA Helicase Reaction. The RNA and DNA substrate components used for these experiments are shown in Figure 1. The synthesis and purification of each have been described under Materials and Methods. The RNA components of the helicase substrates contained both the rho-loading site and the rho-dependent terminator of the *E. coli trp t′* sequence. RNA_{255}, which had been annealed to DNA_{22} at the 3′-end of the RNA (denoted RNA_{255}/DNA_{22}), was used as the helicase substrate in these reactions unless otherwise indicated. The following results were obtained.

(i) Annealing of the Helicase Substrate Goes to Completion. RNA−DNA hybrids were formed by mixing RNA and DNA in 150 mM KCl and slow-cooling the mixture as described under Materials and Methods. The annealing reaction went to completion for RNA_{255} with a 1.6-fold excess of DNA_{22} molecules over RNA. Autoradiographic films of the gels showed no free RNA in the annealing mixture (Figure 2, lanes 2 and 3). Quantitation of the annealing mixtures showed that 90−95% of the RNA chains present were initially annealed to DNA oligomers, as described under Materials and Methods.

(ii) Both ATP and Rho Are Required for Helicase Activity. The helicase reaction requires the presence of hydrolyzable ATP, which was added to the reaction shown in Figure 2 after the sample in lane 3 had been removed. Lane 4 shows that some of the DNA oligomers were removed from the

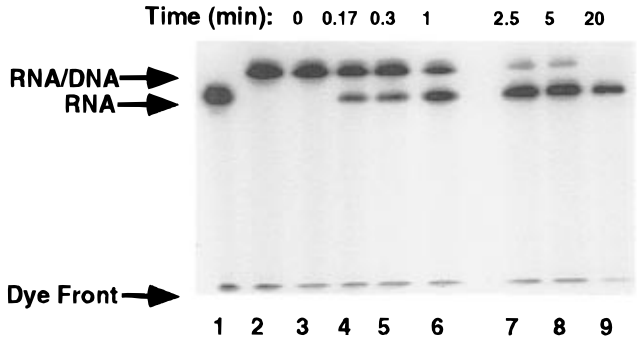

FIGURE 2: Stages of a typical RNA/DNA helicase reaction. Rho hexamers (20 nM) were added to 10 nM RNA_{255}/DNA_{22} helicase substrate and allowed to incubate at 22 °C for 3 min. This reaction was performed in helicase buffer (see Materials and Methods) containing 50 mM KCl. A sample was taken (lane 3) and added to loading buffer containing 1% SDS. Then ATP (1 mM final concentration) was added, and aliquots were removed at the times indicated. Samples were loaded onto a 5.5% Laemmli running gel with a 4% stacking gel (see Materials and Methods) and run at 25 mA for 2 h. The lower band corresponds to free RNA_{255} and the upper band to the RNA_{255}/DNA_{22} hybrid. Lanes 1 and 2 show an RNA_{255} sample and the annealing mixture, respectively, as size markers.

RNA by the rho helicase activity within the first 10 s of the reaction, as demonstrated by the shift of some of the labeled RNA to the lower (free RNA) band. No helicase activity was observed by this criterion in reactions to which no ATP had been added, showing that no DNA was removed from the RNA−DNA substrate in 20 min at 37 °C (data not shown). This indicates that our RNA and rho preparations contained no contaminating ATP, and also that the RNA−DNA hybrid substrates are stable under the gel electrophoresis conditions used.

We also checked the dependence of the helicase activity on the presence of rho. Only 2% of the RNA−DNA substrate molecules were separated in 20 min at 37 °C in the presence of ATP when rho was omitted (data not shown). Therefore, we conclude that the RNA−DNA hybrids were stable under all reaction conditions used except when rho and ATP were both present. These control reactions also contained 60 nM free "trapping" DNA oligomers that were designed to be complementary to the DNA oligomers annealed to the RNA, and thus served to trap the DNA component of the RNA−DNA hybrid when it was released by helicase activity (see below). These control reactions also show that these trapping oligomers do not destablize the RNA−DNA helicase substrate molecules under the reaction conditions of the assay.

(iii) The Helicase Reaction Requires a Rho Loading Site. The RNA that we used for these experiments contains the *trp t′* rho loading site and the termination region from the *trp* operon of *E. coli* (*32*). The loading site falls between residues 28 and 128 of the transcript (numbering from the 5′ end) and contains 27% rC residues and few stable secondary structure elements (hairpin-loops) as defined by a Zuker analysis (*36*), (see Figure 1A). Helicase rates observed with a helicase substrate not carrying an unstructured rho loading site on the RNA were 50-fold slower than the rates observed here (K.M.W., unpublished results).

(iv) The Helicase Reaction Proceeds in the 5′ → 3′ Direction along the RNA. A helicase substrate formed by annealing the DNA oligomer designated $DNA_{20,3'-5'}$ (see Figure 1B) to the 5′-end of the RNA_{255} resulted in very little helicase activity (data not shown). Approximately 0.5 nM of the $DNA_{20,3'-5'}$ oligomer was removed from the RNA_{255} portion of the helicase substrate by 20 nM rho after 40 min. We calculate that 6×10^{-4} DNA oligomers per minute per rho hexamer were removed in this reaction, compared to an initial reaction rate of 2 DNA oligomers removed per minute per rho hexamer with DNA_{22} annealed to the 3′-end of RNA_{255} (see below). We note that the initial reaction rate for the forward reaction has been estimated here in order to compare it with the reverse reaction rate. For the actual data analysis, the forward reaction rate constant was determined by fitting the data to an exponential process as described under Materials and Methods.

We conclude that the forward (5′ → 3′) reaction is >3000-fold faster than the reverse (3′ → 5′) reaction. Only the 5′ → 3′ reaction is analyzed in the following sections.

(v) Helicase Reactions Are Unchanged over a Wide Range of Rho and RNA Concentrations. Previous helicase experiments were performed with 1 nM RNA and 1−10 nM rho hexamers (*6*, *27*), while our experiments were performed with 10−20 nM RNA and 5−20 nM rho hexamers. In order to confirm that our helicase reactions gave similar results to those of Platt and co-workers at the same RNA and enzyme concentrations, we performed control experiments with 1 nM RNA and 1 or 2 nM rho hexamers. We found that the helicase reactions at 1 nM RNA and 1 or 2 nM rho hexamers were very similar to those at 10 nM RNA and 10 or 20 nM rho hexamers, respectively (data not shown). We also performed helicase reactions at 20 nM RNA and 20 nM rho hexamer concentrations and found that the results were similar to those obtained with 10 nM RNA and 10 nM rho hexamers (data not shown). This shows that our results are general for a wide range of rho and RNA concentrations and ratios. We discuss the quantitation of rho binding to RNA in these assays in more detail in the companion paper (*30*).

The qualitative characteristics of the rho-dependent RNA−DNA helicase reaction described above are in full accord with those observed earlier by Platt and co-workers (*6*). We proceed now to analyze the reaction quantitatively to determine the rates of the individual steps of the reaction.

Rho Binding to RNA Is Rapid. Order of addition experiments were performed to isolate possible rate-limiting steps in the helicase reaction. In some experiments, rho was prebound to the helicase substrate molecule, and the reaction was started by adding ATP. In other experiments, ATP was included in the solution containing the helicase substrates, and rho was added to start the reaction. No differences in reaction kinetics were observed (data not shown), indicating that the rho−RNA binding step is not rate-limiting in 50 mM KCl-containing solutions at the concentrations of reactants used. All the reactions described subsequently in this study were initiated by the addition of ATP.

The Helicase Reaction Has Two Phases. The loading buffer used to stop the helicase reaction, as well as the gels within which the samples were run, contained SDS (see Materials and Methods). As a consequence, rho is denatured at the time the samples are taken, and thus can be separated from the nucleic acid components of the helicase reaction. This means that the upper and lower RNA bands in the gel contain the nucleic acid substrate components that had been released at the time the sample was removed from the helicase reaction, as well as those that were bound to rho.

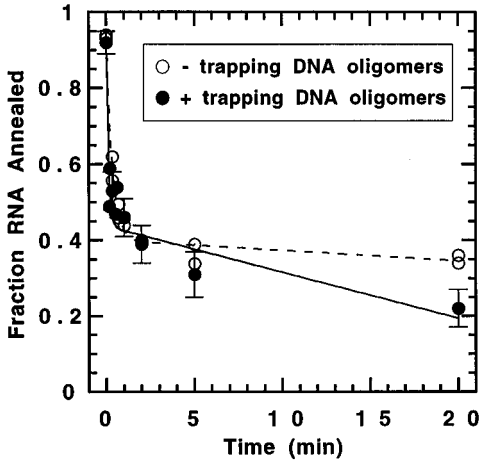

FIGURE 3: Slow phase of the helicase reaction. 10 nM RNA_{255}/DNA_{22} helicase substrate was incubated with 10 nM rho in the presence (solid circles) or absence (open circles) of a 60 nM concentration of complementary DNA oligomers in 50 mM KCl. Samples at various times were quenched and run on a gel as shown in Figure 2. The solid lines show the best fit of the data to eq 1. Symbols with error bars indicate averaged data for six separate experiments. Symbols without error bars represent individual measurements.

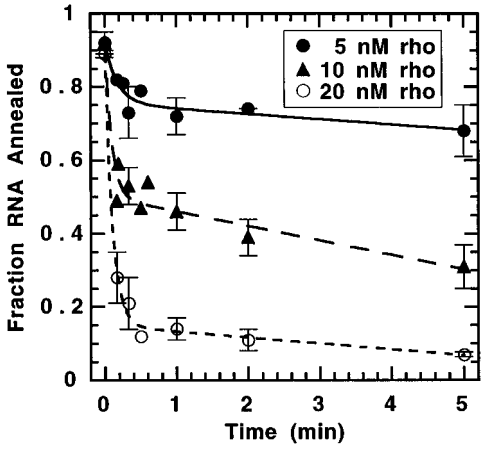

FIGURE 4: Helicase reaction at different rho to helicase substrate concentration ratios. Helicase reactions were performed with 10 nM RNA_{255}/DNA_{22} substrate and 5−20 nM rho hexamers at 37 °C (5 nM rho, solid circles; 10 nM rho, solid triangles; 20 nM rho, open circles). The data are fit to the sum of one exponentially-decaying function plus a linear term (see eq 1). The values for the amplitude and rate constant of the exponential phase from the fits for these reactions are shown in Table 1. Isolated symbols indicate individual measurements or the averaged value for two measurements, and the error bars show the standard deviation at points for which three or more measurements were made. The data for the 10 nM rho experiments over a longer time interval are also shown in Figure 3.

In Figure 3 (and subsequent plots of the helicase reaction data), we graph the fraction of RNA that is annealed to the complementary DNA oligomer as a function of time. Figure 3 shows that the helicase kinetics consist of two phases when the reaction is run in 50 mM KCl. The first phase decays exponentially, while the second phase decays much more slowly and can be represented as a linear process (eq 1).

Various experiments were performed to characterize the reactions responsible for each of the kinetic phases observed. We will show that the fast reaction is important for understanding how rho interacts with the helicase substrate. In contrast, the slow phase is a complex combination of secondary reactions that include the dissociation of rho from RNA, the reannealing of DNA oligomers to the RNA, and the recycling of rho to other RNA molecules.

DNA Oligomers Can Rebind to the RNA Substrate during the Helicase Reaction. In early experiments we found that the helicase reaction did not go to completion because the second phase of the reaction was very slow (Figure 3). In fact, in some reactions the fraction of RNA substrate molecules bound to DNA decreased initially and then appeared to increase again after 20−30 min of incubation (data not shown). We interpreted this to mean that the DNA oligomers released by the helicase reaction were rehybridizing to the RNA during the second phase of the reaction. This hypothesis was tested by adding an excess of "trapping" DNA oligonucleotides complementary to the DNA_{22} that had been annealed to the RNA in forming the original helicase substrate. Trapping DNA oligomers were routinely added to the reaction before the addition of rho or ATP.

Figure 3 shows that the second phase of the reaction appears to become faster in the presence of 60 nM trapping DNA oligomer. This concentration of trapping oligomers is enough to bind all of the extra DNA present in the original RNA−DNA annealing reaction (see Materials and Methods) and to leave a 5-fold excess of trapping oligomer in the reaction solution. Under these conditions, the DNA_{22} oligomers freed from the RNA substrate hybridize preferentially with the added trapping DNA, both because the latter is present in much higher concentrations than the released RNA component of the substrate and because the free RNA can form intrachain secondary structure that could inhibit the rebinding of the released DNA. As a consequence, the second phase of the helicase reaction appears to be faster since the reverse reaction (i.e., reannealing of DNA oligomers to RNA) was inhibited by the trapping DNA oligomers.

Control experiments confirmed that the two complementary DNA oligomers can form duplex molecules under the helicase assay conditions used. A helicase reaction was performed with unlabeled RNA annealed to unlabeled DNA, to which we added ^{32}P-labeled trapping DNA oligomers. The formation of a radioactively-labeled band at the correct molecular weight for the expected DNA duplex was observed (data not shown). In addition, as stated above, this concentration of trapping DNA oligomers does not displace DNA from the RNA−DNA helicase substrate. Control rho−RNA binding experiments were performed in which trapping DNA oligomers were added to the final concentration prior to the addition of rho. The presence of these oligomers did not interfere with the binding of rho to the RNA rho-loading site (data not shown).

Characterization of the Burst Phase. We performed experiments to define the steps of the helicase reaction that occur during the burst phase. We show (see below) that this phase corresponds to a single round of the helicase reaction. In addition, our results demonstrate that the stoichiometry of rho hexamer binding to the RNA_{255} substrate is 2 to 1 under our standard helicase reaction conditions.

We examined the amplitude of the helicase reaction at 37 °C as a function of the molar ratio of helicase substrate to rho by using a fixed 10 nM concentration of helicase substrate and varying the concentration of rho hexamers from 5−20 nM. The helicase kinetics show that the amplitude of the fast phase of the reaction increases as the relative concentration of rho is increased (Figure 4). In contrast, we

Table 1: Amplitudes and Rate Constants of the First Phase of the Helicase Reaction at Different Rho Concentrations[a]

[rho hexamers] (nM)	[rho]/[RNA]	RNA	amplitude[b]	rate constant[c]
5	0.5	RNA_{255}	0.17 ± 0.04	6 ± 5
10	1.0	RNA_{255}	0.41 ± 0.03	11 ± 4
20	2.0	RNA_{255}	0.73 ± 0.03	10 ± 2
10	1.0	RNA_{255}+(rC)[d]	0.43 ± 0.04	7 ± 2
20	2.0	RNA_{255}+(rC)[d]	0.67 ± 0.04	14 ± 4
10	1.0	RNA_{391}	0.27 ± 0.05	4 ± 2
20	2.0	RNA_{391}	0.57 ± 0.05	5 ± 1

[a] Results obtained from helicase reactions shown in Figures 4, 5, and 7. Reaction conditions were 50 mM KCl, 10 nM RNA, 37 °C. Errors were obtained from fits to eq 1 (Materials and Methods). [b] The amplitude is given as the fraction of DNA oligomers removed in the first phase of the reaction. [c] Units are min^{-1}. [d] Reactions contained 1−3 mM poly(rC) (concentration units are rC residues).

also found that the rate constant of the fast phase of this reaction was (within experimental error) unchanged in these experiments (Table 1). In the companion paper (*30*), we show that each rho hexamer binds to RNA in an approximately 1 to 1 molar ratio when the rho hexamer concentration is 0.2 nM. We did not carry out extensive helicase assays at these concentrations because rho hexamers dissociate under these conditions (*9*, *12*) and lose ATPase activity in 5−10 min (data not shown). As a consequence, our assays were routinely performed at equal molar concentrations (∼10 nM) of helicase substrate and rho hexamer.

If the 1:1 RNA to rho hexamer binding stoichiometry also applied at equal concentrations of rho and RNA, we would expect all the substrate molecules to bind a rho hexamer. As a consequence, the helicase reaction should go to completion (unwind all the substrate molecules) in a single burst phase. However, under 1:1 concentration conditions, we observe that the helicase reaction slows down and enters the second (slow) phase after only about half of the annealed DNA oligomers have been released (Figures 3 and 4 and Table 1). Since we have shown that all the rho hexamers are fully active as helicases (see *30*), this result suggests that more than one rho hexamer must be binding per RNA rho loading site under these conditions. This result is fully consistent with our earlier observation that rho binds to poly(rC) and other polyribonucleotides with moderate cooperativity (*37*, *38*).

The loading site of the *trp t′* transcript on the RNA_{255} helicase substrate is slightly atypical, in that it is contained within a region that is effectively unstructured over ∼180 nt (Figure 1A). An unstructured region of this length surrounding the loading site should be able to bind two (or even three) rho hexamers simultaneously, since the site size for the binding of a single rho hexamer is 60−80 nt (*37*, *38*). In the companion paper (*30*), we use a combination of rho−RNA binding and ATPase measurements to show that 2−3 rho hexamers bind to each RNA_{255}-containing substrate under the conditions used in our helicase reactions and that ∼4 bind to each RNA_{391}-containing substrate.

Reactions with a Rho Trap. As indicated above, we have postulated that the first phase of the helicase reaction corresponds to a single round of rho helicase activity. To test this proposal, we added 1−3 μM (in rC residue units) poly(rC) to the reaction as a rho trap at the same time as the ATP was added to initiate the reaction. As a consequence, any rho released from the RNA helicase substrate would be captured, and thus the reaction should be confined to a single cycle of helicase activity. Poly(rC) was used as a rho trap because this polynucleotide binds to rho particularly tightly (*18*, *37*). We found that while the first phase of the helicase reaction was unaffected by poly(rC), the slow phase was completely inhibited (Figure 5) and that the trapping effect of poly(rC) was independent of poly(rC) concentration over the range tested (Figure 5). These results show that the second phase of the helicase reaction corresponds to processes that occur after the first (burst) phase has gone to completion. In addition, since the first phase was unaffected by poly(rC), these results show that poly(rC) does not actively displace rho hexamers from the RNA_{255} helicase substrate during the burst phase.

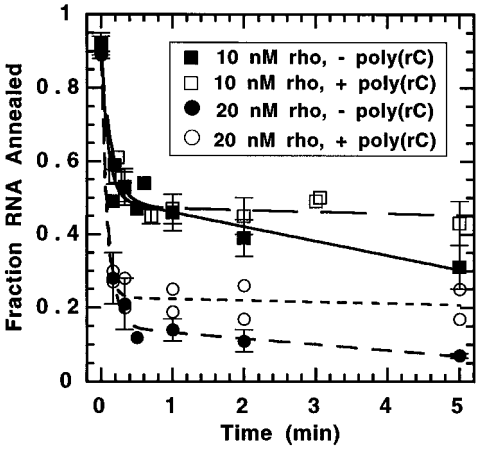

FIGURE 5: Time course of the helicase reaction in the presence and absence of a poly(rC) trap. RNA−DNA hybrids (10 nM) were incubated with either 10 nM rho (squares) or 20 nM rho (circles). 1 mM ATP was added at the start of the reactions represented by solid symbols. For the reactions represented by open symbols, ATP was added together with 1−3 μM poly(rC) trap (concentrations in rC residue units). The lines represent the best fit to eq 1, and the amplitudes and rates of the first phase of the data are shown in Table 1. Symbols with error bars correspond to the average value and standard deviation for three or more measurements. Isolated symbols represent individual measurements. The data in solid symbols are also shown in Figure 4.

As described above, complementary DNA oligomers designed to trap the released DNA_{22} molecules were added to all of the helicase reactions to prevent DNA reannealing. Therefore, both the reannealing reaction and the rho rebinding reaction were inhibited in these protocols. Since poly(dC) binds to rho as tightly as poly(rC), but does not activate the rho ATPase (*37*, *39*), we tested poly(dC) as a rho trap and found that it was just as effective as poly(rC) (data not shown). We used long (>300 nt) poly(rC) and poly(dC) chains for these experiments because shorter chains did not completely inhibit the slow phase of the reaction (data not shown).

The Slow Phase of the Rho Helicase Reaction. In this section, we show that the rate of RNA release from rho is very slow in 50 mM KCl, and that rho can recycle during the helicase reaction if the RNA release rate is increased.

(i) The Slow Phase Reflects Slow Release of the RNA Portion of the Helicase Substrate from Rho after the Helicase Reaction (DNA Release) Is Complete. The helicase reaction slows down after the burst phase, indicating the presence of a rate-limiting step in second (and subsequent) rounds of the rho-catalyzed reaction. We know that this slow step occurs after the separation of the RNA−DNA hybrid because

we see a burst of DNA release. A slow step earlier in the reaction pathway would give rise to single-phase reaction kinetics that would continue until equilibrium had been reached. Previous workers have found that RNA is released from rho slowly in 50 mM KCl (*29*, *40*). Thus, we suspected that the release of rho from the RNA portion of the helicase substrate after DNA release might represent the slow step of the reaction.

This hypothesis was tested by measuring the rate of RNA release from rho. We found that the off-rate of RNA from rho is 0.036 (±0.006) min^{-1} and 0.024 (±0.006) min^{-1} in 50 mM KCl in the absence or presence of 1 mM ATP, respectively (data not shown). The off-rate of RNA from rho had been previously measured in 50 mM KCl and found to be 0.02 min^{-1} (*29*, *40*), also in the presence or the absence of ATP. The off-rate of RNA from rho is ~300-fold slower than the rate constant of the first phase of the helicase reaction (6−14 min^{-1}, Table 1). Therefore, rho must recycle very slowly, and the overall helicase reaction exhibits a burst phase followed by a much slower process (or set of processes). Note that the helicase reactions were carried out at 37 °C, while the RNA off-rate measurements were performed at 22 °C (see Materials and Methods). The helicase reaction proceeds similarly at 22 °C and at 37 °C, except that the rate constant of the burst phase is ~5-fold slower at the lower temperature (see Figure 5B in ref *30*).

(ii) The Slow Phase of the Helicase Reaction Is Largely Eliminated in 150 mM KCl. We wished to determine whether rho can recycle (i.e., can act catalytically) in the helicase reaction. The experiments with and without a poly(rC) trap described above (Figure 5) show that rho can recycle slowly in 50 mM KCl, because the second phase of the reaction is completely inhibited by trapping the released rho with poly(rC). Since we found that the RNA release rate is very slow in 50 mM KCl, we sought conditions under which the helicase reaction could still occur but with a faster rate of RNA release from rho. Others have found that the binding (association) constant of rho to RNA decreases as the concentration of KCl increases (*29*, *41*), suggesting that under these conditions one might expect the rate of dissociation of RNA from rho to increase. We tested this hypothesis by raising the monovalent salt concentration in the helicase assay to 150 mM KCl, because rho still binds to RNA reasonably well under these conditions. At still higher KCl concentrations, the binding of rho to RNA is very weak, and the helicase reaction is very slow and inefficient (data not shown).

Using RNA release experiments at 150 mM KCl, we found that 40−45% of the RNA was released at a rate of 9 (±8) and 3 (±2) min^{-1} in the absence and presence of ATP, respectively (data not shown). Since this rate of RNA release from rho is 100-fold faster than that seen in 50 mM KCl, we performed helicase reactions in 150 mM KCl with excess RNA to test for recycling of rho under these higher salt conditions (Figure 6). We found that a reaction containing twice as much RNA as rho consists of a single exponentially-decaying phase that goes to completion (Figure 6, solid circles). Under these conditions, it appears that the rate of the helicase reaction is similar to the rate of RNA release, permitting rho to recycle rapidly and the reaction to go to completion in a single phase. The catalytic helicase reaction is discussed in more detail below.

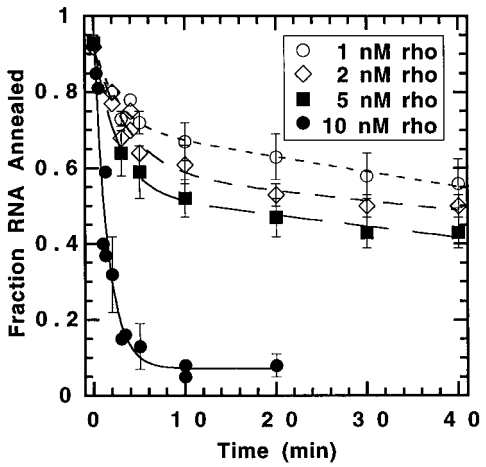

FIGURE 6: Catalytic rho helicase reaction. Helicase reactions were performed with 20 nM RNA_{255}/DNA_{22} substrate and with 1 nM (open circles), 2 nM (open diamonds), 5 nM (solid squares), or 10 nM (solid circles) rho hexamers in helicase buffer containing 150 mM KCl. The data were fit to a single-exponential curve plus a constant term (for the 10 nM data) or plus a linear term (for the 1−5 nM data). The results of these fits are shown in Table 2. Symbols with error bars represent average values for three to five individual measurements. Isolated symbols represent single measurements.

(iii) The Slow Phase of the Helicase Reaction Is Due to Side Reactions. The slow phase of the helicase reaction is a complex combination of side reactions that do not yield much information on either the helicase reaction or the mechanism of rho translocation. The apparent rate of the slow phase is decreased by the reannealing of released DNA to the RNA substrate. This reannealing can be prevented by the addition of complementary DNA oligomers to trap the DNA oligomers released from the helicase substrate. The rate of the slow phase of the helicase reaction is also limited by the slow rate of RNA release from rho. As indicated above, at low salt concentration (50 mM KCl), this slow step causes the helicase reaction to exhibit pre-steady-state burst kinetics. Such kinetics are observed when the first round of a reaction is rapid and is then followed by a slow (rate-limiting) step (e.g., slow product release or slow substrate rebinding).

We showed above that the first round of the helicase reaction reflects the movement of rho from the rho loading site to the 3′-end of the RNA molecule, accompanied by the release of the DNA oligomer that had been annealed to the RNA. Since rho does not bind to DNA oligomers as well as to the long RNA molecules of the helicase substrate, it is likely that rho removes and releases the complementary DNA oligomers rapidly from the RNA portion of the helicase substrate, and that the subsequent release of the free RNA is slow. We conclude that a fraction of the annealed DNA oligomers is removed rapidly from the RNA portion of the helicase substrate during the burst phase of the reaction in 50 mM KCl, while the release of the rest of the DNA oligomers reflects the rate-limiting release of rho from the RNA and rebinding to a new helicase substrate that still carries hybridized DNA.

Catalytic Helicase Reaction. Since we found that rho releases RNA rapidly in 150 mM KCl, we performed helicase reactions to test for catalytic activity with 2−20-fold as much RNA−DNA substrate as rho hexamers (Figure 6). We found that rho completely removes all the hybridized DNA oligo-

Table 2: Amplitudes and Rate Constants of Both Phases of the Catalytic Helicase Reaction[a]

[rho hexamers] (nM)	A_1[b]	k_1[c]	A_2[d]	k_2[e]
1	0.22 ± 0.04	0.4 ± 0.1	0.71 ± 0.03	0.004 ± 0.001
2	0.33 ± 0.06	0.3 ± 0.1	0.59 ± 0.06	0.003 ± 0.002
5	0.39 ± 0.03	0.38 ± 0.06	0.53 ± 0.02	0.003 ± 0.001
10	0.90 ± 0.06	0.7 ± 0.1	0.07 ± 0.04	0

[a] Data in Figure 7 were fit to eq 1. Reactions were performed at 37 °C in helicase buffer containing 150 mM KCl and 20 nM RNA_{255}/DNA_{22}. [b] Amplitude of the exponential phase (given as the fraction of DNA oligomers removed in this phase). [c] Rate constant of the exponential phase (units min^{-1}). [d] *Y* intercept of the linear phase. [e] Slope of the linear phase (fraction DNA oligomers removed per minute).

mers in reactions containing twice as much helicase substrate as rho hexamers. In helicase reactions with 4−20-fold as much substrate as rho (Figure 6), the reaction slowed down after 10 min. In the reaction with 20-fold as much substrate as rho, each rho hexamer recycled about 8 times in 40 min. This shows that each rho hexamer has the capacity to separate more than one RNA−DNA hybrid if the rate of release of rho from the RNA substrate is rapid.

The rate of the catalytic helicase reaction is slower than that of the fast phase of the reaction in 50 mM KCl (compare the rates of the total reaction in Figure 6 and Table 2 with the rates of the burst phase shown in Figure 3 and Table 1). Elsewhere (K.M.W., unpublished results) we use single-round experiments to show that the helicase reaction in 150 mM KCl is slower because rho translocates along the RNA more slowly and because rho increasingly dissociates from the RNA before reaching the RNA−DNA hybrid region (i.e., rho translocates along the RNA less processively at the higher KCl concentrations). We showed above that the rates of the burst phase of helicase reactions in 50 mM KCl are independent of rho concentration, indicating that only one round of the helicase reaction is occurring. In contrast, the catalytic rate decreases somewhat with decreasing rho concentrations in the 5−10 nM rho hexamer concentration range. Therefore, it appears that under catalytic reaction conditions the RNA component of the helicase substrate may release and rebind rho hexamers multiple times during a single cycle of the helicase reaction.

The rate of the catalytic reaction in 150 mM KCl is partially determined by the rate of rho binding, and thus is somewhat dependent on rho and RNA concentrations (see above), as well as on the rate of RNA release from rho and the rate of translocation of rho along the RNA. On the other hand, the rate of the helicase reaction at rho concentrations from 1−5 nM is almost constant (Table 2). This indicates that when the ratio of RNA to rho is greater than 4:1, a slow step in the reaction begins to limit the rate of the reaction. We assume that eventually RNA release becomes rate-limiting even at this higher KCl concentration.

Interpretation of the Rate of the Burst Phase. We showed above that the burst phase of the helicase reaction occurs before rho protein recycles onto a second RNA molecule. We also showed that the burst phase has the same rate constant, whether the reaction is started with rho or with ATP, and that this rate constant is independent of the concentration of rho. These results indicate that the reaction steps during the burst phase occur after rho binding, but before release of the RNA product of the reaction. These reaction steps include rho translocation from the rho loading site to the DNA oligomer and the subseqent release of the complementary DNA oligomer from the helicase substrate by rho.

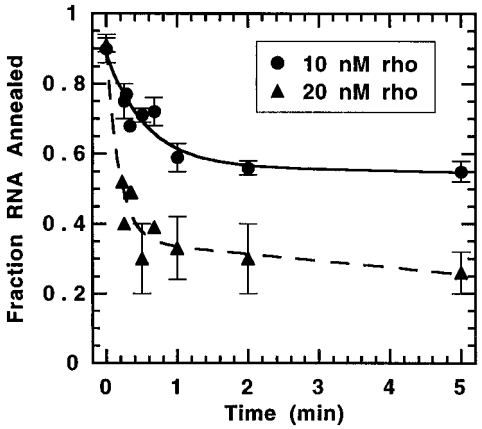

FIGURE 7: Helicase reactions with the RNA_{391}/DNA_{20} helicase substrate. Helicase reactions were performed with 10 nM RNA_{391}/DNA_{20} substrate and 10 (solid circles) or 20 (solid triangles) nM rho at 37 °C in helicase buffer containing 50 mM KCl. The data were fit to eq 1, and the results of the fits to the exponential phase are shown in Table 1. The symbols with error bars show average values for three or more data points measured under the same conditions. Symbols without error bars represent individual measurements.

Processive movement of rho from one end of the RNA molecule to the other could, in principle, occur by a number of mechanisms, including tracking along the RNA, as well as by direct transfer by looping out of the intervening portion of the RNA strand. Previous experiments have shown that rho can separate RNA−RNA duplexes at high (4 mM), but not at low (0.4 mM) Mg^{2+}, concentrations (*27*). Platt and co-workers took advantage of this property to construct a helicase substrate with a 50 bp RNA−RNA duplex between the rho loading site and a 28 bp RNA−DNA duplex (*28*). They found that the RNA−DNA duplex was only disrupted under high Mg^{2+} concentration conditions, where the upstream RNA−RNA duplex could also be disrupted. This showed that rho cannot bypass a 50 bp hybrid structure located between the rho loading site and an annealed DNA oligomer.

If rho does indeed translocate along the RNA molecule, it should take longer to reach a DNA oligmer that is located at the 3′-end of a longer RNA molecule. To test this hypothesis, we performed experiments with a longer RNA substrate (RNA_{391}) annealed to DNA_{20} (Figure 7). This RNA includes the entire sequence of RNA_{255} at the 5′-end with added plasmid-encoded sequences at the 3′-end (see Figure 1A) that contain part of the coding sequence of the *lacZ* gene. [Note that the added *lacZ* sequences do not include those important for rho-dependent termination in the *lacZ* operon as determined by Ruteshouser and Richardson (*42*).] There is almost no helicase activity with only this 3′ portion of RNA_{391} (data not shown) since it does not contain a rho loading site. We conclude that rho interacts initially with the RNA_{391} substrate at the same loading site used in the RNA_{255} substrate.

The reaction profiles of the helicase reactions with either the RNA_{255}/DNA_{22} or the RNA_{391}/DNA_{20} substrate are similar in 50 mM KCl (compare Figure 4 with Figure 7). Both reactions show two kinetic phases, indicating that the slow release of RNA from rho is limiting the recycling of

rho. This is consistent with rho−RNA binding measurements that show that rho binds very tightly to RNA_{391} (data not shown). The amplitudes of the burst phase of the reactions with RNA_{391} in 50 mM KCl are slightly smaller than the amplitudes of the reactions with RNA_{255} (Table 1). This may reflect the additional cooperativity of binding of rho hexamers to this longer RNA. We find that ∼4 rho hexamers bind to RNA_{391} under our standard assay conditions (see ref *30*), consistent with the longer length of this RNA transcript.

The average rate constant of the burst phase with the RNA_{255} substrate is 9 (±3) min^{-1} (Table 1, Figure 4). The average rate constant of the burst phase with the RNA_{391} substrate is 4.5 (±1.5) min^{-1} (Table 1, Figure 7). Thus, the reaction with the longer substrate appears to be somewhat slower, suggesting that the rate constant of the burst phase of the reaction does provide some measure of how rapidly rho translocates along the RNA of the helicase substrate. This issue is considered further in the Discussion.

We attempted to use additional RNA substrates for studying the RNA length-dependence of the helicase reaction rate constant. To this end, helicase experiments were performed with a shorter (127 nt) RNA that only contained the *trp t′* rho loading site (data not shown). This RNA did not bind to rho as well as did the longer substrates, presumably as a consequence of its shorter length. The reaction kinetics for this substrate showed three phases: the burst phase, a rho-recycling phase, and an equilibrium phase. The amplitude of the burst phase was small, and the rate constant was too fast to measure. In the companion paper (*30*), we show experiments with RNA_{255} with a 100 bp RNA−DNA hybrid, for which the DNA component is separated from the RNA more rapidly than for the RNA_{255}/DNA_{22} hybrid shown here. The upstream end of the longer hybrid is closer to the rho loading site of RNA_{255}, and since it is removed more rapidly, this observation is also consistent with the hypothesis that the rate constant of the burst phase measures the rate of rho translocation from the loading site to the upstream end of the RNA−DNA hybrid.

The translocation processes and the RNA−DNA separation processes of the helicase reaction comprise consecutive reactions. Since rho does not move backward (i.e., 3′ → 5′, see above) and since the trapping DNA oligomers prevent re-formation of the RNA−DNA hybrid, both reactions are irreversible. The translocation reaction itself presumably consists of a sequence of consecutive steps. If each intermediate in the translocation reaction forms and decays at similar rates, we would expect to see a lag phase before the separation of the RNA−DNA hybrid because these intermediates would not have reached the RNA−DNA hybrid when the reaction is quenched. We did not observe a lag when we performed experiments with 5 s time points (data not shown), indicating that the intermediates in the translocation reaction form and decay at different rates (*43*). This is in contrast to the results of Ali and Lohman (*44*), where they did observe a lag phase in the DNA unwinding reaction with UvrD, a DNA helicase from *E. coli*. It is possible that translocation through a double-stranded DNA substrate is more uniform than along an RNA substrate, since RNA can form complex double-stranded secondary structure.

DISCUSSION

Characterization of the Reaction. In this paper, we have described the kinetics of the RNA−DNA helicase reaction catalyzed by transcription termination factor rho. This reaction has two phases at low salt concentration (50 mM KCl). We have shown that the slower phase represents a combination of side reactions, which include RNA release from rho, DNA reannealing to the RNA substrate, and rho recycling onto other RNA molecules. The reannealing reaction can be inhibited by trapping the released DNA oligomers with complementary oligomers as they are released from the RNA by rho (Figure 3), and the recycling of rho can be inhibited by adding poly(rC) or poly(dC) as a rho trap (Figure 5). A single round of the helicase reaction can thus be isolated by using these traps in combination.

Rate of Rho Translocation. We have shown that the first phase of the helicase reaction corresponds to the time required for rho to translocate from the loading site to the DNA oligomer. The RNA in most of these experiments was 255 nt in length and contained a rho loading site located between RNA positions 28 and 128. If rho interacts with all of the nucleotide residues located between the rho loading site and the 3′-end of the RNA (∼130 nt), then the rate of translocation along the RNA (∼20 nt/s) can be calculated from the average rate constant of the first phase of the helicase reaction (∼9 min^{-1}, Table 1). For the RNA_{391} substrate, which contains the same loading site in the same position as the RNA_{255} substrate, the average rate of translocation estimated on this same basis is also ∼20 nt/s. The fact that these estimates are the same for both RNA substrates is consistent with the hypothesis that the rate constant of the first phase of the helicase reaction measures the average rate of rho translocation along the RNA substrate. We emphasize that the actual translocation reaction is probably not monotonic, and that the distance traveled is likely to be influenced by RNA secondary structure, because rho may translocate past RNA hairpins without unwinding them (see Discussion in *30*).

We can compare the effective translocation rates estimated above with the rates of RNA synthesis that have been measured by others. The rate of synthesis by *E. coli* RNA polymerase, and thus the rate of translocation of the transcription complex along the DNA template *in vivo*, is ∼40 nt/s at 37 °C (*45*). This rate is also achieved *in vitro* at nucleotide triphosphate concentrations above ∼1 mM. Others have suggested that salts such as KGlu or KOAc may simulate the *in vivo* environment more closely than KCl (*46*). In addition, the intracellular Mg^{2+} concentration is closer to 5 mM than the 1 mM we used in these studies. We found that the rate constant of the first phase of the helicase reaction in 5 mM $MgCl_2$ and 50 mM KOAc is about 2-fold slower than that in 1 mM $MgCl_2$ and 50 mM KCl (K.M.W., unpublished results). We conclude that rho translocates along the nascent transcript at ∼25% of the rate at which the transcription complex moves along the DNA template under reaction conditions comparable to those in the cell. Since rho must, at least, contact the transcription complex in order to trigger termination, this suggests that the elongating polymerase complex must pause in order for rho to "catch-up" with it.

Early experiments showed that rho-dependent termination sites are generally RNA polymerase pause sites (*21*−*23*).

Our results are consistent with the hypothesis that the positions of rho-dependent terminators are, at least partially, determined by the relative rates at which rho translocates along the RNA transcript and RNA polymerase translocates along the DNA template (*24*). Other results show that the efficiency of rho-dependent termination is not always proportional to the lengths of pauses of the transcription complex at defined template sites, suggesting that other factors are also important in controlling rho-dependent termination efficiency (*47*; A. Q. Zhu and P. H. von Hippel, in preparation).

The Catalytic Helicase Reaction. Earlier experiments (*27*−*29*) had shown that, under the conditions tested, wild-type rho seemed only to act as a stoichiometric helicase. We attribute this to the fact that RNA binds tightly to rho under these reaction conditions (which were very similar to those of our 50 mM KCl system), and that therefore rho does not release the RNA substrate rapidly enough to recycle. We have shown that rho releases RNA much more rapidly in 150 mM KCl. Therefore, we performed the helicase reaction with more RNA−DNA helicase substrate than rho hexamers at this salt concentration and found that wild-type rho can indeed act as a catalytic RNA−DNA helicase. Brennan and Platt (*29*) studied the helicase reaction with a mutant rho protein that binds RNA weakly and showed that the mutant could function catalytically as a helicase at 50 mM KCl. Their result is consistent with the hypothesis that rho can act catalytically in the helicase reaction if it releases the RNA product of the reaction sufficiently rapidly.

The helicase reactions that we have studied at 50 and 150 mM KCl describe two points of a continuum of helicase activity as a function of increasing salt concentration. At low salt, rho binds tightly to the RNA substrate, translocates rapidly, and separates one RNA−DNA hybrid per reaction. At intermediate salt concentrations (∼150 mM), rho binds more weakly to the RNA, translocates more slowly and less processively (K.M.W., unpublished results), and acts catalytically. This illustrates a trade-off. In order for rho to translocate rapidly and processively along the RNA, it must bind tightly to the RNA component of the helicase substrate. However, it does not recycle under these conditions. In order for rho to act catalytically, it must release each RNA product rapidly, but rho is also less processive under these conditions (K.M.W., unpublished results) because it can dissociate from the RNA transcript before it reaches the DNA oligomer located at the 3′-end of the RNA. This shows that the reaction conditions, and not the intrinsic properties of rho protein, determine the kinetic profile of the helicase reaction. The rho helicase reaction must be studied carefully under different conditions to define reaction mechanisms.

Macromolecular crowding occurs in the intracellular environment, and the concentration of K^+ is high while that of Cl^- is low. These conditions would probably increase the strength of the rho−RNA binding interaction and tend to make rho translocation more processive. The rho-dependent termination sites on the *trp t′* transcript occur upstream of where DNA was annealed to our helicase substrate (*48*, *49*), so rho does not have to translocate as far on this transcript *in vivo* to cause termination as it does to separate the RNA−DNA hybrid in our experiments. Reactions formulated to better simulate the intracellular environment (i.e., in KOAc, KGlu, and at higher Mg^{2+} concentrations) are described in detail elsewhere (K.M.W., J.M.D., and P.H.v.H., in preparation).

One aspect of the helicase reaction of rho that has not been explicitly considered is that the "bare" RNA product of the helicase reaction binds to rho as well as does the initial helicase substrate (*30*). This is expected because rho makes its primary binding interaction with the rho loading site of the RNA (*17*). After the first round of the helicase reaction, bare RNA can act as a competitive inhibitor because rho may bind to and translocate along bare RNA molecules before binding to a substrate that still carries an RNA−DNA hybrid. Product inhibition may also limit the ability of rho to recycle during the helicase reaction. We found that rho can recycle up to 8 times in 150 mM KCl (Figure 6), but this reaction also eventually slows down.

ACKNOWLEDGMENT

We thank members of our laboratory for helpful discussions and Professor Terry Platt (University of Rochester) for plasmids p39ASE and pWU5.

REFERENCES

1. Richardson, J. P. (1996) *J. Biol. Chem. 271*, 1251−1254.
2. Bear, D. G., and Peabody, D. S. (1988) *Trends Biochem. Sci. 13*, 343−347.
3. Yager, T. D., and von Hippel, P. H. (1987) in *E. coli and S. typhimurium: Cellular and Molecular Biology* (Neidhardt, F. C., Ed.) pp 1241−1275, American Society of Microbiology, Washington, D.C.
4. Platt, T., and Richardson, J. P. (1992) in *Transcriptional Regulation* (McKnight, S. L., and Yamamoto, K. R., Eds.) pp 365−388, Cold Spring Harbor Laboratory Press, Plainview, NY.
5. Platt, T. (1994) *Mol. Microbiol. 11*, 983−990.
6. Brennan, C. A., Dombroski, A. J., and Platt, T. (1987) *Cell 48*, 945−952.
7. Nudler, E., Mustaev, A., Lukhtanov, E., and Goldfarb, A. (1997) *Cell 89*, 33−41.
8. Finger, L. R., and Richardson, J. P. (1982) *J. Mol. Biol. 156*, 203−219.
9. Geiselmann, J., Yager, T. D., Gill, S. C., Calmettes, P., and von Hippel, P. H. (1992) *Biochemistry 31*, 111−121.
10. Geiselmann, J., Yager, T. D., and von Hippel, P. H. (1992) *Protein Sci. 1*, 861−873.
11. Gogol, E. P., Seifried, S. E., and von Hippel, P. H. (1991) *J. Mol. Biol. 221*, 1127−1138.
12. Seifried, S. E., Bjornson, K. P., and von Hippel, P. H. (1991) *J. Mol. Biol. 221*, 1139−1151.
13. Lowery-Goldhammer, C., and Richardson, J. P. (1974) *Proc. Natl. Acad. Sci. U.S.A. 71*, 2003−2007.
14. Morgan, W. D., Bear, D. G., Litchman, B. L., and von Hippel, P. H. (1985) *Nucleic Acids Res. 13*, 3739−3754.
15. Chen, C.-Y. A., and Richardson, J. P. (1987) *J. Biol. Chem. 262*, 11292−11299.
16. Alifano, P., Rivellini, F., Limauro, D., Bruni, C. B., and Carlomagno, S. M. (1991) *Cell 64*, 553−563.
17. Ceruzzi, M. A. F., Bektesh, S. L., and Richardson, J. P. (1985) *J. Biol. Chem. 260*, 9412−9418.
18. Galluppi, G. R., and Richardson, J. P. (1980) *J. Mol. Biol. 138*, 513−539.
19. Geiselmann, J., Wang, Y., Seifried, S. E., and von Hippel, P. H. (1993) *Proc. Natl. Acad. Sci. U.S.A. 90*, 7754−7758.
20. Reisbig, R. R., and Hearst, J. E. (1981) *Biochemistry 20*, 1907−1918.
21. Lau, L. F., Roberts, J. W., and Wu, R. (1983) *J. Biol. Chem. 258*, 9391−9397.
22. Morgan, W. D., Bear, D. G., and von Hippel, P. H. (1983) *J. Biol. Chem. 258*, 9553−9564.
23. Morgan, W. D., Bear, D. G., and von Hippel, P. H. (1983) *J. Biol. Chem. 258*, 9565−9574.

24. Jin, D. J., Burgess, R. R., Richardson, J. P., and Gross, C. A. (1992) *Proc. Natl. Acad. Sci. U.S.A. 89*, 1453−1457.
25. Greenblatt, J., McLimont, M., and Hanly, S. (1981) *Nature 292*, 215−220.
26. Yang, X. J., and Roberts, J. W. (1989) *Proc. Natl. Acad. Sci. U.S.A. 86*, 5301−5305.
27. Brennan, C. A., Steinmetz, E. J., Spear, P., and Platt, T. (1990) *J. Biol. Chem. 265*, 5440−5447.
28. Steinmetz, E. J., Brennan, C. A., and Platt, T. (1990) *J. Biol. Chem. 265*, 18408−18413.
29. Brennan, C. A., and Platt, T. (1991) *J. Biol. Chem. 266*, 17296−17305.
30. Walstrom, K. M., Dozono, J. M., and von Hippel, P. H. (1997) *Biochemistry* (following paper in this issue).
31. Nehrke, K. W., Seifried, S. E., and Platt, T. (1992) *Nucleic Acids Res. 20*, 6107.
32. Wu, A. M., Christie, G. E., and Platt, T. (1981) *Proc. Natl. Acad. Sci. U.S.A. 78*, 2913−2917.
33. Chamberlin, M. J., and Patterson, D. L. (1965) *J. Mol. Biol. 12*, 410−428.
34. Ts'o, P. O. P., Rapaport, S. A., and Bollum, F. J. (1966) *Biochemistry 5*, 4153−4170.
35. Wong, I., and Lohman, T. M. (1993) *Proc. Natl. Acad. Sci. U.S.A. 90*, 5428−5432.
36. Zuker, M., and Stiegler, P. (1981) *Nucleic Acids Res. 9*, 133−148.
37. McSwiggen, J. A., Bear, D. G., and von Hippel, P. H. (1988) *J. Mol. Biol. 199*, 609−622.
38. Bear, D. G., Hicks, P. S., Escudero, K. W., Andrews, C. L., McSwiggen, J. A., and von Hippel, P. H. (1988) *J. Mol. Biol. 199*, 623−635.
39. Seifried, S. E., Easton, J. B., and von Hippel, P. H. (1992) *Proc. Natl. Acad. Sci. U.S.A. 89*, 10454−10458.
40. Steinmetz, E. J., and Platt, T. (1994) *Proc. Natl. Acad. Sci. U.S.A. 91*, 1401−1405.
41. Faus, I., and Richardson, J. P. (1989) *Biochemistry 28*, 3510−3517.
42. Ruteshouser, E. C., and Richardson, J. P. (1989) *J. Mol. Biol. 208*, 23−43.
43. Gutfreund, H. (1995) *Kinetics for the Life Sciences. Receptors, Transmitters, and Catalysts*, Cambridge University Press, Cambridge, England.
44. Ali, J. A., and Lohman, T. M. (1997) *Science 275*, 377−380.
45. Vogel, U., and Jensen, K. F. (1994) *J. Bacteriol. 176*, 2807−2813.
46. Leirmo, S., Harrison, C., Cayley, D. S., Burgess, R. R., and Record, M. T., Jr. (1987) *Biochemistry 26*, 2095−2101.
47. Richardson, L. V., and Richardson, J. P. (1996) *J. Biol. Chem. 271*, 21597−21603.
48. Zalatan, F., and Platt, T. (1992) *J. Biol. Chem. 267*, 19082−19088.
49. Zalatan, F., Galloway-Salvo, J., and Platt, T. (1993) *J. Biol. Chem. 268*, 17051−17056.

BI963179S